The flexibility matrix of timber composite beams with a discrete connection system

Jose L. Fernandez-Cabo
Associate Professor, UPM
Technical University of Madrid (UPM), Spain
jose.fcabo@upm.es

Jorge Fernandez-Lavandera
Agricultural Ing. PhD. Ciete Ingenieros
Madrid, Spain
jorge@ciete.es

Rafael Diez-Barra
Researcher Ph.D.; INIA-CIFOR
Madrid, Spain
diez@inia.es

Jose M. Avila-Jalvo
Associate Professor, UPM
Madrid, Spain
3307avila@coam.es

Keywords – Timber composite beams, discrete connection system, flexibility matrix

ABSTRACT

This work presents a method for the analysis of timber composite beams which considers the slip in the connection system, based on assembling the flexibility matrix of the whole structure. This method is based on one proposed by Tommola and Jutila (2001). This paper extends the method to the case of a gap between two pieces with an arbitrary location at the first connector, which notably broadens its practical application. The addition of the gap makes it possible to model a cracked zone in concrete topping, as well as the case in which forming produces the gap. The consideration of induced stresses due to changes in temperature and moisture content is also described, while the concept of *equivalent eccentricity* is generalized.

This method has important advantages in connection with the current European Standard EN 1995-1-1: 2004, as it is able to deal with any type of load, variable section, discrete and non-regular connection systems, a gap between the two pieces, and variations in temperature and moisture content. Although it could be applied to any structural system, it is specially suited for the case of simple supported and continuous beams.

Working examples are presented at the end, showing that the arrangement of the connection notably modifies shear force distribution. A first interpretation of the results is made on the basis of the *strut and tie* theory. The examples prove that the use of EC-5 is unsafe when, as a *rule of thumb*, the *strut* or compression field between the support and the first connector is at an angle with the axis of the beam of less than 60^0.

1. Introduction

Annex B of the current European Standard EN 1995-1-1: 2004 (EC-5) applies the *Gamma* method first proposed by Möhler (Möhler, 1956) to the analysis of timber composite beams. An explanation of the method can be found in Ceccotti (1995) and Kreuzinger (1995). The method is based on an approximated solution of the differential equation of the problem, by considering a cosine (or sine) load function instead of a uniformly distributed load.

The *Gamma* method offers an elegant solution with good exactitude for simple supported beams with smeared connections, uniform cross section and uniformly distributed load. Additionally, the *Gamma* coefficient is quite a good illustration of the nature of the problem.

Nevertheless, the said assumptions are quite restrictive. Moreover, as Girhammar et al. (2007) pointed out, use of this method in cantilevers as allowed by EC-5 gives erroneous results. Girhammar (2009) also presented a simplified method based on the exact formulation in 2007.

An important current trend covers connection systems that use discrete and stiffer connectors such as notches, while the *Gamma* method is unable to properly address this problem.

Matrix and Finite Element analysis methods were first developed for steel-concrete composite beams (e.g. Salari, 1998; Sebastian, 2000). There was a short delay before they were applied to timber-timber or timber-concrete composite beams, although major work was done in the 1990s (e.g. Amadio, 1990; Amadio et al. 1993; Fragiacomo 2006; Fragiacomo et al. 2006). Current formulations include a local approach, i.e. making a specific FEM model of the connection (e.g. Dias et al. 2007). The analysis of composite beams is still an active research field (e.g. Ranzi et al. 2006, 2010; Sousa Jr. et al 2010 a,b). A more complete state of the art can be found in Lukaszewska (2009) and Fernández-Lavandera (2010).

This paper expands the flexibility method developed by Tommola and Jutila (2001). Their work was developed in the context of the Nordic Timber Bridge Project (Jutila and Salokangas, 2000, 2010). The recently added figures mainly consist of the possibility of a gap between the two pieces and the location of the first connector at an arbitrary position (a very important question, as will be seen in section 3), and not only over the support. The addition of the gap makes it possible to model a cracked zone in concrete topping, as well as the case where forming produces that gap. The means of computing thermal or moisture-induced stresses (only for cases without a gradient across the section of each piece) is described, together with a general description of the concept of *equivalent eccentricity*.

The method is a reasonable combination of generality and simplicity. As the flexibility matrix is obtained for the whole structure, the method cannot be easily applied to complex structures. Nevertheless, it is well suited for cases of simple supported beam and even for the case of continuous beams, which are the most common practical cases. It permits analytical parametrical analysis, which was a crucial factor in considering the method worthy of study.

Section 2 of the paper describes the proposed method of analysis in a detailed form. Section 3 describes working examples and contains the discussion. The selected examples will show that shear force distribution strongly depends on the location of the first connector, as quite different distributions other than those obtained using the *Gamma* method are possible. The discussion links the results with the *strut* and *tie* theory in order to obtain a *rule of thumb* for use where EC-5 is unsafe. Finally, section 4 contains the conclusions.

2. Analysis Method

This section describes the complete procedure for assembling the flexibility matrix of the whole structure, considering the horizontal slip at the connectors to be kinematic variables. It is therefore a particular application of the *flexibility method*. The method is fully implemented for a simple supported beam (fig. 1).

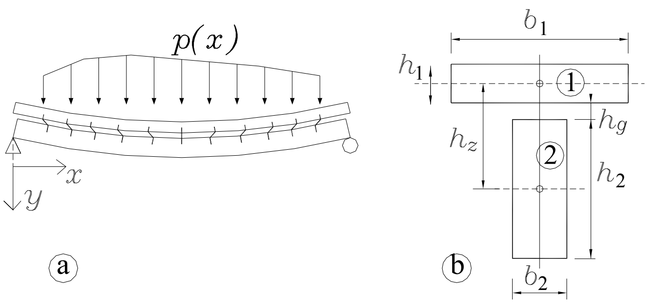

Figure 1 – a) Front view of a beam with the reference axis, and b) transversal type section

The load and cross section can be arbitrary. A gap in the section is considered, which is associated with a non-structural forming of a concrete top or, more important, with the modelling of a cracked area also for a concrete top.

2.1. Assumptions

This analysis is made under the following assumptions:

i) the connection system is discrete and located in an arbitrary position, and its behaviour, i.e. the relation between shear force and the corresponding slip, is linear; friction between the two pieces is not considered.

ii) the Navier–Bernouilli hypothesis used for *strength of materials* is considered valid inside every piece.

iii) the material joining the pieces suffers deformation due only to the shear connection force, and it does not resist normal stresses in the direction of the piece.

iv) deflection is small, and therefore the curvature of the two pieces can be considered equal to that of the beam, and

v) deflection is due only to the bending moment and shear influence is not considered.

2.2. Analysis scheme

The internally static indeterminate structure is divided into two complementary stages (Fig. 2): stage S1, with all but the first left connector, numbered 0 (see Fig. 3), released; and stage S2, considering the effect of the released shear forces (numbered from 1 to *n*, see Fig. 3). If the structure were also externally statically indeterminate, such as for a continuous beam, the procedure would have to include redundant reactions at stage S2.

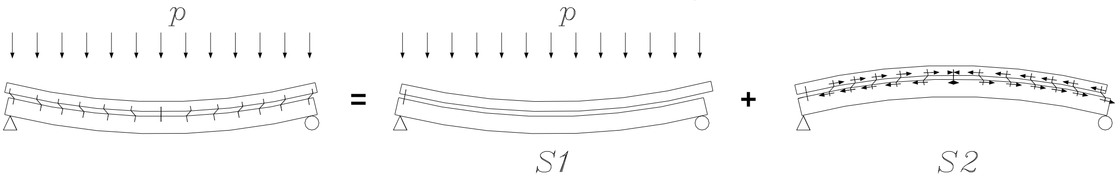

Figure 2 –Division of the analysis in two complementary stages: S1 and S2

Additionally, the superposition principle will be applied in stage S2, as linear behaviour in the materials and in the connection system is considered, and it will be analyzed as the sum of the effect of the *n* individual redundant shear forces.

Final results are only shown for the case of a uniform cross section, uniformly distributed load and two symmetric pieces. The general case can be easily implemented by following the next sections.

2.3. Equivalent eccentricity of the connector shear force

The concept of equivalent eccentricity comes from the field of steel-concrete composite beams (see e.g. Byfield 2002), and it notably simplifies the analysis of stage S2.

The case with vertical dowels will be analyzed first, followed by two current important cases: notches and castellated surfaces. These three cases will make it possible to draw general conclusions.

Fig. 3a shows part of the front view of the beam, with the location of horizontal section A. Section A cuts the connectors along the gap. The position of section A is defined by the variable h_x, and it is placed at the position of null bending moment in the dowel in order to consider only the horizontal shear force. If the connector were rebar at an angle to the horizontal, working in a scheme of *strut and tie*, the cut can be anywhere inside the gap, as there are only axial forces in the rebar. As will be shown, the position of section A, as defined by variable h_x, does not influence the value of the equivalent eccentricity.

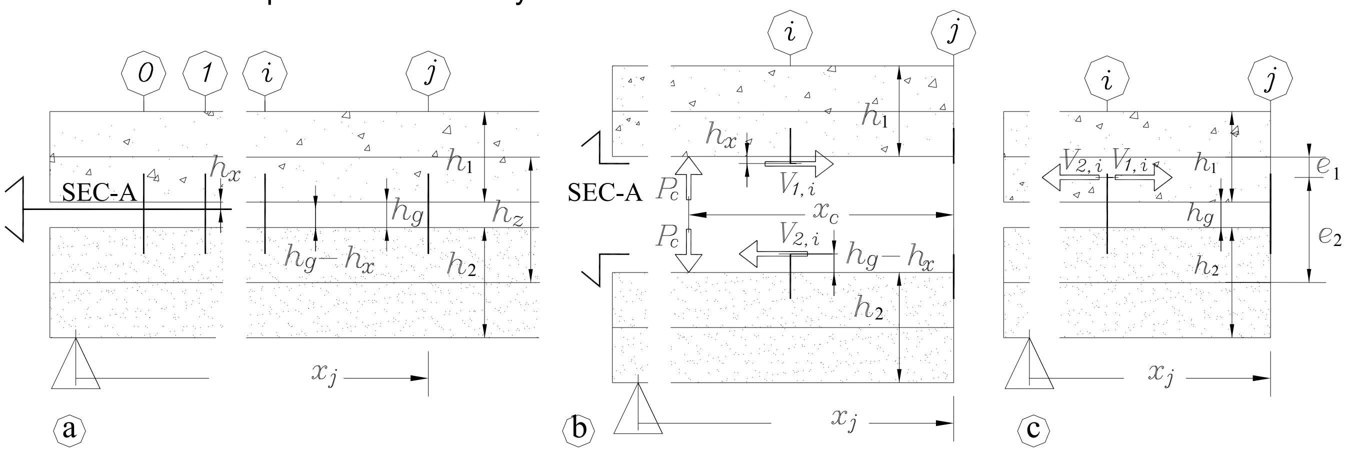

Figure 3 a)Part of the front view of the beam, with the location of section A; b) front view with separation of the two pieces by section A, showing the horizontal shear forces and vertical contact forces for the case of connector i; c) position of the shear forces at the equivalent eccentricity, also for the connector i.

Fig. 3b shows the same front view while separating the pieces by horizontal section A. The resultant of the vertical contact forces, P_c, is located at a distance x_c to section j. The shear forces $V_{1,i}$ and $V_{2,i}$ in connector *i* produce the next bending moments at the centre of gravity of the pieces, e.g., section *j* :

$$V_i \cdot (h_1/2 + h_x) - P_c \cdot x_c \,; \qquad V_i \cdot (h_2/2 + h_g - h_x) + P_c \cdot x_c \quad \text{with } V_i = V_{1,i} = V_{2,i} \tag{1}$$

The moment produced by P_c can be established in terms of the shear force V_i using a new variable termed e_k:

$$P_c \cdot x_c = V_i \cdot e_k\,; \tag{2}$$

According to assumption number iv:

$$\frac{V_i \cdot (h_1/2 + h_x) - V_i \cdot e_k}{D_1} = \frac{V_i \cdot (h_2/2 + h_g - h_x) + V_i \cdot e_k}{D_2} \tag{3}$$

where D_i is the bending stiffness for piece i, and the other terms were defined in Fig. 1 and Fig. 3.

From analysis of eq. 1 and Fig. 3b it can be seen that variable e_k represents a change in the initial eccentricity of the shear forces in comparison with that showed in fig. 3b; i.e. subtracting e_k for $V_{1,i}$ and adding e_k for $V_{2,i}$. The *equivalent eccentricity*, i.e. the eccentricity of the shear force at connectors to avoid the consideration of P_c in the stage S2, can be therefore computed (see fig. 3a and 3c) as:

$$e_1 = h_1/2 + h_x - e_k\,;\quad e_2 = h_2/2 + h_g - h_x + e_k\,;\quad e_1 + e_2 = h_z\,; \tag{4}$$

and the final value can be obtained by solving eq. 3 for e_k and substituting it in eq. 4:

$$e_i = h_z \cdot D_i / (D_1 + D_2)\,;\quad \text{with}\quad i = 1,2 \tag{5}$$

The case without a gap also leads to eq. 5. The couple of shear forces at section i produce, respectively, and at the centre of gravity of pieces 1 and 2 of any section between connector number 0 and i, a normal force V_1 and V_2, and a bending moment $V_1 \cdot e_1$ and $V_2 \cdot e_2$.

Fig. 4 shows the corresponding strain diagram, where two symmetric pieces are considered (i.e. with the neutral axis in the middle of its height).

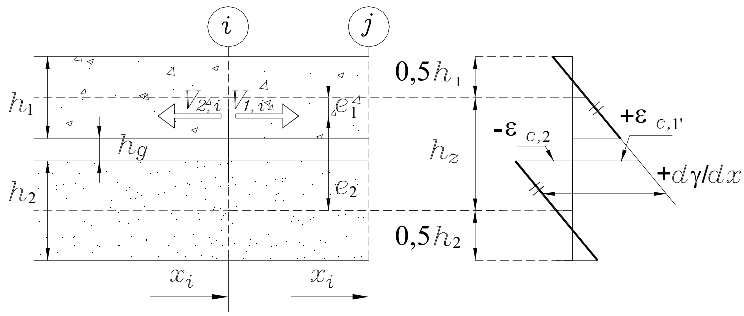

Figure 4 – Equivalent eccentricity of the couple shear forces at connector i and the corresponding strain diagram of any section between connector number 0 and i.

2.4. Slip for the released statically determinate beam: stage S1

Fig. 6 shows the typical strain diagram at any cross section between connector number 0 and j. From equilibrium (note that there is no shear force between the pieces):

$$m_1 + m_2 = M(x) \tag{6}$$

where $M(x)$ is the overall bending moment at that section, and m_i the local bending moment at the centre of gravity of piece i.

Considering eq. 6 and assumption number (iv):

$$m_i = M(x) \cdot D_i / (D_1 + D_2)\,;\ \text{with}\quad i = 1,2 \tag{7}$$

The slip at section j, γ_j, can be obtained by:

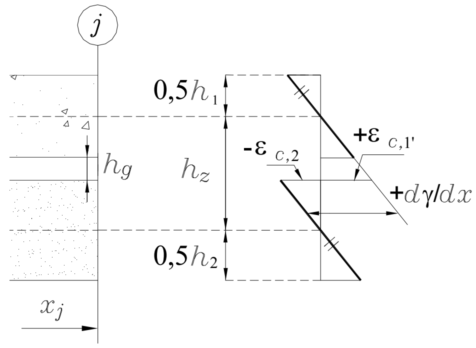

Figure 5 – Typical strain diagram at sections between connector number 0 and j in stage S1 (the sign convention shown for the slip will be used for its final balance in eq. 17)

$$\gamma_j = \int_{x_0}^{x_j} (\varepsilon_{c,1'} - \varepsilon_{c,2}) dx \tag{8}$$

$$\text{with } \varepsilon_{c,1'} = M(x) \cdot (h_1 / 2 + h_g) / (D_1 + D_2) \tag{9}$$

$$\varepsilon_{c,2} = -M(x) \cdot h_2 / 2 / (D_1 + D_2) \tag{10}$$

The sign convention of the slip implicitly defined according to eq. 8 (see also Fig.5) will be used for its final balance in eq. 17.

Eq. 8 can be easily numerically integrated for any load and cross section type; i.e. for a general case. The solution for a uniformly distributed load, p , and a uniform cross section is:

$$\gamma_j = \frac{h_z}{(D_1 + D_2)} \cdot \frac{p}{2} \cdot (L \cdot \frac{(x_j^{\ 2} - x_0^{\ 2})}{2} - \frac{(x_j^{\ 3} - x_0^{\ 3})}{3}) \tag{11}$$

L being the span of the beam.

2.4.1. Thermal or moisture induced stresses

The question of induced stresses will only be introduced here. A detailed and more general explanation is beyond the scope of this paper. Thermal and hygrothermal induced stresses can be easily included at this stage just by adding the contribution due to the temperature and moisture content variations of the two pieces to γ_j. All the other steps remain the same. The method is therefore quite general.

2.5. Slip due to redundant shear forces: stage S2

Slip is evaluated in stage S2 at the location of the redundant connectors, and can be seen as the sum of two components.

The first, stage S2-I, is the slip at section j due to the bending moments produced by the redundant shear forces, $V_{c,i}$ (with i from 1 to n), at the centres of gravity of the two pieces:

$$\sum_{i=1}^{n} V_{c,i} \cdot \gamma_{ji} \tag{12}$$

where γ_{ji} is the slip at section j due to a unitary shear force at section i, $V_{c,i}$ the of total value of the shear force at section i; with (see Fig. 4)

$$\gamma_{ji} = \int_{x_0}^{x_a} (\varepsilon_{c,1'} - \varepsilon_{c,2}) \cdot dx \ + \ \frac{1}{K_{ser,0}} \tag{13}$$

where $K_{ser,i}$ is the equivalent linear stiffness of connector i (see assumption number i).

Using the concept of *equivalent eccentricity* (subsection 2.3), and according to Fig. 4:

$$\gamma_{ji} = \int_{x_0}^{x_a} ((\frac{1}{C_1} + \frac{e_1 \cdot (h_1 / 2 + h_g)}{D_1}) - (-\frac{1}{C_2} - \frac{e_2 \cdot (h_2 / 2)}{D_2}))dx \ + \ \frac{1}{K_{ser,0}} \tag{14}$$

where C_i is the axial stiffness for the piece i and $x_a = \begin{Bmatrix} x_i & if & j > i \\ x_j & if & j \le i \end{Bmatrix}$

The value of γ_{ji} can easily be numerically integrated for any section type, and its result for the case of uniform section is:

$$\gamma_{ji} = (\frac{1}{C_1} + \frac{1}{C_2} + \frac{h_z^{\ 2}}{D_1 + D_2}) \cdot (x_a - x_0) \ + \ \frac{1}{K_{ser,0}}; \tag{15}$$

The second component of the slip, stage S2-II, is the slip at section *j*, considering the stiffness of the connector due to the *unit* shear force at this section:

$$\gamma_{c,j} = 1 / K_{ser,j} \tag{16}$$

2.6. Flexibility matrix

The flexibility matrix is assembled using the compatibility equations at all the n redundant connectors while setting a total null slip value for the sum of all the existing stages (i.e. S1, S2-I and S2-II):

$$\underbrace{\gamma_j}_{stage\,S1} + \underbrace{\sum_{i=1}^{n} V_{c,i} \cdot \gamma_{ji}}_{stage\,S2-I} + \underbrace{V_{c,j} \cdot \gamma_{c,j}}_{stage\,S2-II} = 0\,; \quad j = 1..n \tag{17}$$

The unknowns are the redundant shear forces, $V_{c,i}$ (with i from 1 to n), and therefore:

$$\sum_{i=1}^{n} V_{c,i} \cdot \gamma_{ji} \quad + \quad V_{c,j} \cdot \gamma_{c,j} \quad = \quad -\gamma_j \tag{18}$$

or in matrix form:

$$\begin{bmatrix} \gamma_{11} & \gamma_{12} & \cdots & \gamma_{1n} \\ \gamma_{21} & \gamma_{22} & \cdots & \gamma_{21} \\ \cdots & \cdots & \cdots & \cdots \\ \gamma_{n1} & \gamma_{n2} & \cdots & \gamma_{nn} \end{bmatrix} \cdot \begin{bmatrix} V_{c,1} \\ V_{c,2} \\ \cdots \\ V_{c,n} \end{bmatrix} + \begin{bmatrix} 1/K_{ser,1} & 0 & \cdots & 0 \\ 0 & 1/K_{ser,2} & \cdots & 0 \\ \cdots & \cdots & \cdots & \cdots \\ 0 & 0 & \cdots & 1/K_{ser,n} \end{bmatrix} \cdot \begin{bmatrix} V_{c,1} \\ V_{c,2} \\ \cdots \\ V_{c,n} \end{bmatrix} = \begin{bmatrix} -\gamma_1 \\ -\gamma_2 \\ \cdots \\ -\gamma_n \end{bmatrix} \tag{19}$$

$$\underbrace{\begin{bmatrix} \gamma_{11} + 1/K_{ser,1} & \gamma_{12} & \cdots & \gamma_{1n} \\ \gamma_{21} & \gamma_{22} + 1/K_{ser,2} & \cdots & \gamma_{21} \\ \cdots & \cdots & \cdots & \cdots \\ \gamma_{n1} & \gamma_{n2} & \cdots & \gamma_{nn} + 1/K_{ser,n} \end{bmatrix}}_{[F]} \cdot \underbrace{\begin{bmatrix} V_{c,1} \\ V_{c,2} \\ \cdots \\ V_{c,n} \end{bmatrix}}_{\{V\}} = \underbrace{\begin{bmatrix} -\gamma_1 \\ -\gamma_2 \\ \cdots \\ -\gamma_n \end{bmatrix}}_{-\{\gamma\}} \tag{20}$$

the redundant shear forces can be then calculated by solving this linear system of equations:

$$\underbrace{[F]}_{n\times n}\underbrace{\{V\}}_{n\times 1} = -\underbrace{\{\gamma\}}_{n\times 1} \quad \rightarrow \quad \underbrace{\{V\}}_{n\times 1} = -\underbrace{[F]^{-1}}_{n\times n} \cdot \underbrace{\{\gamma\}}_{n\times 1} \tag{21}$$

The shear force at the first connector, termed 0, can then be obtained considering the general horizontal equilibrium.

It must be noted that the influence of the slip of the connectors is not only reflected at the main diagonal of the flexibility matrix, $[F]$, but also in all the slip terms γ_{ji}, due to the slip of the first connector numbered 0 (see eq. 14 and 18).

It should also be emphasised that if all of the terms $(1/K_{ser,j})$ were removed, the resulting equations would be used for a composite beam without slip at the connection system (see Byfield, 2002 for example).

3. Working examples and discussion

This section develops selected examples to illustrate the application of the model described in section 2 and, additionally, to show how the location of the first connector, termed 0, notably modifies shear force distribution. The examples do not form a complete parametrical analysis as this is not the main focus of this work, but they clearly illustrate the nature of the problem. The application of the *strut and tie* theory will make it possible to obtain a *rule of dumb* for use when EC-5 is unsafe.

3.1. General input data and considerations

The beam used by Tommola and Jutila (2001), a simple supported beam with a uniformly distributed load, was also used as a starting point here in order to compare results.

Two section types were analyzed, case 1 (fig. 6, no gap) and case 2 (fig. 7, a gap of h_g =70mm), with a span L = 20m; a total of 21 discrete connectors; load p =50 kN/m; a total depth of the beam $h = (h_1 + h_g + h_2)$ =1.4m; a concrete top with a width of b_1 = 3m, a depth of h_1 = 0,2m, and a Young modulus of E_1 =30000 N/mm^2; a lower *glulam* beam with a width of b_2 = 0,8m and E_2 =10000 N/mm^2.

The original problem is here additionally expanded using four different locations of the first connector. Three different stiffnesses of the connection system are also used. Thermal or moisture induced stresses are not considered.

The gap would be produced, in this case, by the forming of the concrete topping. In this case the existence of a gap affects the stiffness of the connector when vertical dowels are used (e.g., see Gelfi et al., 2002), but this is not the case for rebar at 45 degrees, which is the system commonly used in the bridges built in Finland.

For the sake of simplicity all of the examples consider a connection system with the same stiffness for each connector (even though the method allows arbitrary values), but this value was adjusted for the same unitary stiffness of the connection system, $k_{unit} = K_{ser} / s$, where s is the separation between connectors. The use of k_{unit} allows comparison of the different arrangements. Three different values for k_{unit} were used: 100, 1000 and 10000 kN/mm/m. The connectors, always 21, were located symmetrically from the centre of the span while varying the spacing between connectors, s; which modifies the distance from the left support to the first connector, x_0:

s = 0,85m→ x_0 = 1,5m; s = 0,9m→ x_0 = 1m; s = 0,95m→ x_0 = 0,5m; s = 1m→ x_0 = 0m.

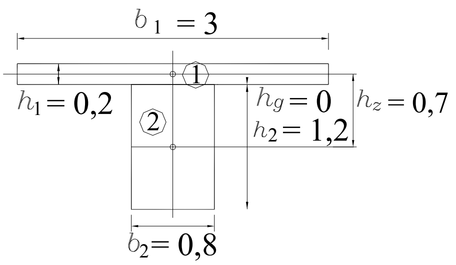

Figure 6 Case 1: section type without gap (measurements in meters)

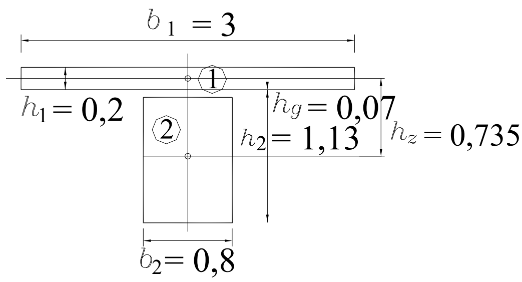

Figure 7 Case 2: section type with 70mm gap (measurements in meters)

3.2. Results for case 1: gapless section

The shear force distributions of the left half of the beam, for case 1 (section without gap, see fig. 8), are shown in figs. 8 to 11. Shear force is plotted in ordinates and the distance from the left support in abscises. A line joints all the discrete values with the same k_{unit} for a better visualization of the results.

Fig. 8 plots the shear forces for a separation between connectors of s = 1m, which means a distance from the left support to the fist connector of x_0 = 0m. The shear force distribution for the lowest value of unitary stiffness, k_{unit} =100 kN/mm/m, presents a typical shape. But as the stiffness is increased, a *lag* at the first connector appears. Fig. 8 shows also that the higher the stiffness, the higher the *lag*. This *lag* is surprising, and it is not detected by the *Gamma* method of EC-5.

Fig. 9 shows the results for a separation between connectors of s = 0,95m, which means a distance from the left support to the first connector of x_0 = 0,5m. These curves basically fit with the application of the *Gamma* method of EC-5.

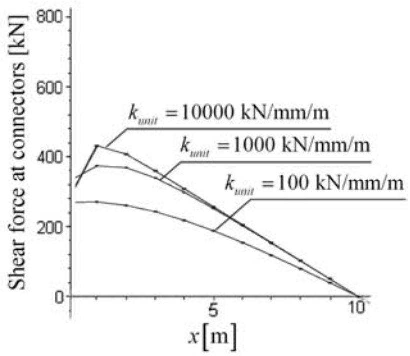

Figure 8 Shear force at connectors (kN) versus distance from the left support: case 1, h_g = 0 m, s = 1 m→ x_0 = 0 m

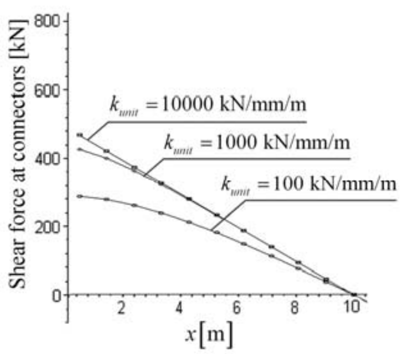

Figure 9 Shear force at connectors (kN) versus distance from the left support: case 1, h_g = 0 m, s = 0,95 m→ x_0 = 0,5 m

Fig. 10 shows the results for a separation between connectors of s = 0,9m, which means a distance from the left support to the first connector of x_0 = 1 m. Fig. 11 shows the results for a separation between connectors of s = 85m, which means a distance from the left support to the first connector of x_0 = 1,5m.

These two plots present a typical shape for the lowest stiffness, k_{unit} =100 kN/mm/m; but for the other two higher values, an opposite tendency appears in comparison with the first case of s = 1m (Fig. 8); I.e., a notable increase in the shear force at the first connector (which will be termed *advance*). In parallel with the first case of s = 1m, Fig. 8 shows that the greater the stiffness, the greater the *advance*. This phenomenon cannot also be detected using the *Gamma* method of EC-5.

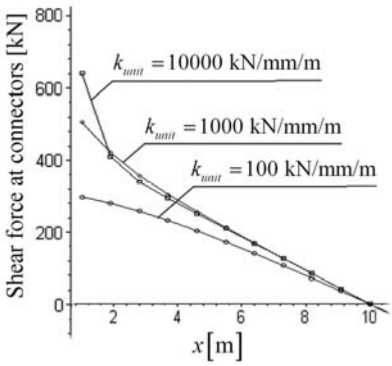

Figure 10 Shear force at connectors (kN) versus distance from the left support: case 1, h_g = 0 m, s = 0,9 m→ x_0 = 1 m

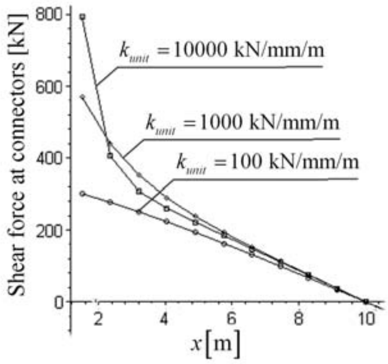

Figure 11 Shear force at connectors (kN) versus distance from the left support: case 1, h_g = 0 m, s = 0,85 m→ x_0 = 1,5 m

3.3. Results for case 2: section with a gap of 70 mm

A gap of 70mm (see fig. 9) does not merely influence the results. In comparison with the results shown in Figs. 10 to 13 for case 1 without a gap, only a light increase in the shear force is detected.

Only one case in Fig. 14 is therefore plotted, the case with the biggest difference, corresponding to s = 0,85m→ x_0 = 1,5m. The criteria for plotting this figure are the same as those described in sub-section 3.2 for case 1.

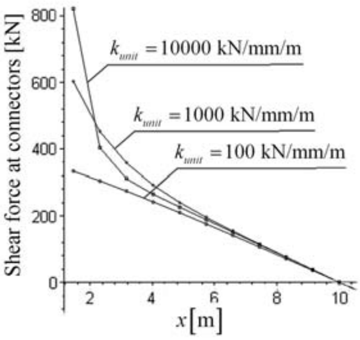

Figure 12 Shear force at connectors (kN) versus distance from the left support: case 2, h_g = 0,07 m, s = 0,85 m→ x_0 = 1,5 m

3.4. Discussion

The results shown in sub-sections 3.2 and 3.3 illustrate the remarkable influence of the location of the first connector on shear force distribution. As was pointed out, the use of the EC-5 model does not detect this, as it leads to a shear force distribution similar to that of Fig. 9 (s = 0,95 m→ x_0 = 0,5 m).

A first or intuitive explanation of the results can be made on basis of the *strut and* tie model (see for example Schlaich et al. 1987 and Muttoni et al. 1997). It must be remembered that the Navier–Bernouilli assumptions are not valid when, as close the supports, there is a quick change in the stress field.

The reaction at the supports produces, as internal forces, one *tie* or tension field and a *strut* or compression field forming an optimal angle α each other in the range of $30^0 \le \alpha \le 60^0$.

The *lag* shown in Fig. 8 (s = 1m→ x_0 = 0m) corresponds to a *strut* of $\alpha \le 90^0$, and therefore the first connection is introduced before the optimal angle $30^0 \le \alpha \le 60^0$. This would explain the delay in the shear force.

A typical shear distribution such as the one shown in Fig. 9 (s = 0,95 m→ x_0 = 0,5 m) corresponds to a *strut* of around $\alpha \leq 64^0$, approximately in the optimal range. This seems also to fit with the regular shear distribution.

The *advance* shown in Fig. 11 and Fig. 12 (s = 0,85m→ x_0 = 1,5m) corresponds with a *strut* of around $\alpha \leq 35^0$, which is beginning to be out of the optimal values of $30^0 \leq \alpha \leq 60^0$, and which would explain the *advance* in connection with a delay in the introduction of the connection.

The *advance* shown in Fig. 10 (s = 0,9m→ x_0 = 1m) corresponds to a *strut* of around $\alpha \leq 46^0$, still in the optimal range, and therefore the existing *advance* cannot be explained using this reasoning.

The question of the *advance* is particularly relevant in the field of refurbishment, where timber beams often present decay close to the support, and due to contact with a masonry wall. If a composite beam were then made, the first connector would necessarily be subjected to a far higher shear force than the second one.

On other hand, the slight variation in the results with and without a gap is explained because the gap is small and located at the web. Nevertheless, from a practical point of view, and as was remarked above, it would not be so easy or may even be impossible to keep the stiffness values with the gap, depending in the type of connector.

4. Conclusions

A method for assembling the flexibility matrix of a timber composite beam with a discrete connection system, considering the slip at the connectors, has been presented. The method improves a previous one proposed by Tommola and Jutila (2001), as it considers an arbitrary position of the first connector and a possible gap between the two pieces of the mixed beam. This improvement considerably broadens its practical application. The consideration of thermal or moisture induced stresses was also remarked on, and the concept of *equivalent eccentricity* was described in general.

This method can easily deal with any load and type of cross section, any location and stiffness of a set of discrete connectors; but it is chiefly suitable for simple supported or continuous beams, which are very important cases in practice. Even though other more general approaches are possible, this method, being simple, is an important improvement over the *Gamma* method described in annex B of EC-5.

Working examples were developed for a beam similar to that used by Tommola and Jutila (2001), and the cases were expanded around two section types: without and with a gap of 70mm. A total of 21 connectors were uniformly distributed except for the location of the nearest connector to the supports, placed at a distance of 0; 0,5; 1 and 1,5 m. Three different stiffnesses of the connectors were analyzed. A constant total depth of the beam and the same unitary stiffness of the connection were used in order to compare the different cases.

The working examples show how important the position of the first connector is, as it can notably modify shear force distribution. A typical shear force distribution corresponds, as a *rule of thumb*, with the location of the first connector at a distance from the supports of around half the depth of the lower piece of the beam. When the first connector is located before that position, there is an *advance* in the shear force for it; and the higher the stiffness of the connection system, the higher the *advance*. When the first connector is placed over the supports, there is a *lag* in the shear force for it; and the higher the stiffness of the connection system, the higher the *lag*.

They also show that the use of EC-5 is unsafe when, as a *rule of thumb*, the *strut* or compression field between the support and the first connector is at an angle with the axis of the beam of less than 60^0. However, additional detailed studies are clearly needed, given that a complete parametrical study was not undertaken.

Acknowledgements

The results presented here were developed under the research project: "*Definition of a protocol for the refurbishment of timber floors by connecting with new concrete topping*", carried out with the financial support of the Spanish Government within the R&D-2004 National Research Program (reference number BIA2004-07317).

Bibliographic References

Amadio, C. (1990). “Elementi finite per lo studio flessionale elatico di travi composte di connessioni deformabili.” *Costruzioni Metalliche* 6, 365–374.
Amadio, C. y Fragiacomo, M. (1993). “A finite element model for the study of creep and shrinkage effects in composite beams with deformable shear connections”. *Costruzioni Metalliche* 4, 213-228.
Byfield, M.P.(2002). “Analysis of composite beams with widely spaced shear connectors”. *The Structural Engineer*. 2 July, 2002.
Ceccotti, A. (1995). “Lecture E13: Timber-concrete composite structures.” *STEP 2. Timber engineering*, Centrum Hout, The Netherlands,E13/1-12.
Dias, A. M. P. G.; Van de Kuilen, J.W.; Lopes S.; Cruz, H. “A non-linear 3D FEM model to simulate timber–concrete joints”. *Advances in Engineering Software* 38 (2007) 522–530.
EN 1995-1-1: 2004. Comité Européen de Normalisation (CEN). “Eurocode 5—Design of timber structures—Part 1-1: General rules and rules for buildings”. Brussels, Belgium (see amendments in ENV 1995-1-1: 2004/A1: 2008)
Fernandez-Lavandera, Jorge (2010). “Mixed Structure with Timber: Efficiency for a Flexible Connection”. Ph.D. Thesis (in Spanish) (to be presented in January 14th 2011). Technical University of Madrid.
Fragiacomo, M., and Ceccotti, A. (2006). “Long-term behaviour of timber-concrete composite beams. I: Finite element modelling and validation.” *J. Struct. Eng.*, 132,1, 13–22.
Fragiacomo, M. (2006). “Long-term behaviour of timber-concrete composite beams. II: Numerical analysis and simplified evaluation.” *J. Struct. Eng.*, 132,1, 23–33.
Gelfi, P., Giuriani, E., and Marini, A. (2002). “Stud shear connection design for composite concrete slab and wood beams.” *J. Struct. Eng*.,128_12_, 1544–1550.
Girhammar, U. A.; Pan Dan, H. (2007). “Exact static analysis of partially composite beams and beams-columns”. *International Journal of Mechanicals Sciences* 49 (2007), 239-255.
Girhammar, U. A. (2009). “A simplified analysis method for composite beams with interlayer slip”. *International Journal of Mechanical Sciences* 51 (2009), 515-530.
Jutila, A.; Salokangas, L. (2000). “Research on and Development of Wooden Bridges in Finland”. *Structural Engineering International* 3, 182-185.
Jutila, A.; Salokangas, L. (2010). “Wood-Concrete Composite Bridges Finish Speciality in the Nordic Countries”. In *Proceedings of the Int. Conference on Timber Bridges*, Lillehammer, Norway. Edited by Malo, K.A.; Kleppe, O. and Dyken T. pp. 383-392.
Kreuzinger, H. (1995). “Lecture B11: Mechanically jointed beams and columns.” *STEP 1. Timber engineering*, Centrum Hout, The Netherlands, B11/1-8.
Lukaszewska, E. (2009). Development of Prefabricated Timber-Concrete Composite Floors. Doctoral Thesis. Luleå University of Technology. Printed by Universitetstryckeriet, Luleå 2009.
Möhler, K. (1956). Über das Tragverhalten von Biegerträgern und Druckstäben mit zusammengestezten Querschnitten und nachgiebigen Verbindungsmitteln. Habilitation, Technische Universität Karlsruhe, Germany.
Muttoni, A., Schwartz, J. y Thürlimann, B. (1997). *Design of concrete structures with stress fields*, Birkhaüser/Springer, 1997, 145p.
Salari, R. M., Spacone, E., Shing, P. B., and Frangopol, D. (1998). “Nonlinear analysis of composite beams with deformable shear connectors.” *J. Struct. Eng*., 124 10, 1148–1158.
Sebastian W. M.; McConnel R.E. (2000) “Nonlinear FE Analysis of Steel-concrete Composite Structures”. *J. Struct. Eng.*, 124 10, 1148–1158.
Ranzi, G.; Gara, F. (2006). “General method of analysis for composite beams with longitudinal and transverse partial interaction”. *Computers and Structures* 84, 2373-2338.
Ranzi, G.; Dall´Astra, A.; Ragni, L. y Zona, A. (2010). “A geometric nonlinear model for composite beams with partial interaction”. *Engineering Structures* 32, 1384-1396.
Schlaich, J., Schäfer, K. y Jennewein, M. (1987).“Toward a consistent design of structural concrete“, *PCI. Journal*, May-June, 1987, 75-150.
Sousa Jr., J. B. M.; da Silva, R.A. (2010a). “Analytical and numerical analysis of multilayered beams with interlayer slip. *Engineering Structures* 32 (2010), 1671-1680.
Sousa Jr., J. B. M.; Oliveira, C.E.M.; da Silva R.A. (2010b). “Displacement-based nonlinear finite element analysis of composite beam-columns with partial interaction”. J*ournal of Construction Steel Research*, 66 (2010) 772-779.
Tommola, J.; Jutila, A. (2001). “Analysis of Wood-Concrete Composite Girder with Discrete Shear Connectors”. *Proceedings of the IABSE conference on Innovative Wooden Structures and Bridges;* Lathi, Finland; August 29-31, 293-296.